JACS
JOURNAL OF THE AMERICAN CHEMICAL SOCIETY

Subscriber access provided by American Chemical Society

Communication

Reversible Control of Free Energy and Topography of Nanostructured Surfaces

Qiang Fu, G. V. Rama Rao, Solomon B. Basame, David J. Keller, Kateryna Artyushkova, Julia E. Fulghum, and Gabriel P. Lpez

J. Am. Chem. Soc., **2004**, 126 (29), 8904-8905• DOI: 10.1021/ja047895q • Publication Date (Web): 03 July 2004

Downloaded from http://pubs.acs.org on March 31, 2009

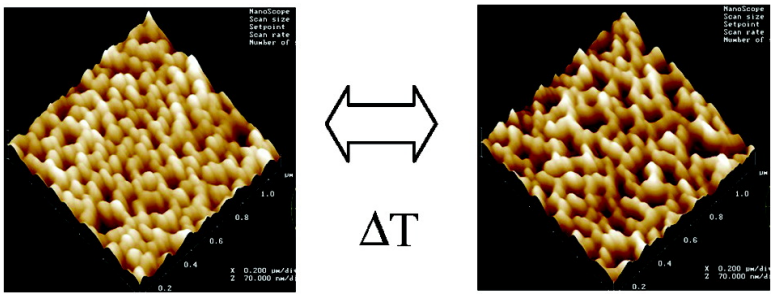

More About This Article

Additional resources and features associated with this article are available within the HTML version:

- Supporting Information
- Links to the 11 articles that cite this article, as of the time of this article download
- Access to high resolution figures
- Links to articles and content related to this article
- Copyright permission to reproduce figures and/or text from this article

View the Full Text HTML

ACS Publications
High quality. High impact.

Journal of the American Chemical Society is published by the American Chemical Society. 1155 Sixteenth Street N.W., Washington, DC 20036

J|A|C|S
COMMUNICATIONS

Published on Web 07/03/2004

Reversible Control of Free Energy and Topography of Nanostructured Surfaces

Qiang Fu,[‡] G. V. Rama Rao,[†] Solomon B. Basame,[‡] David J. Keller,[‡] Kateryna Artyushkova,[†] Julia E. Fulghum,[†,‡] and Gabriel P. López*[,†,‡]

Center for Micro-Engineered Materials, Department of Chemical and Nuclear Engineering, and Department of Chemistry, The University of New Mexico, Albuquerque, New Mexico 87131

Received April 12, 2004; E-mail: gplopez@unm.edu

There has been considerable interest recently in the development of materials whose surface properties can be modulated dynamically. A method of choice has been through the use of stimuli responsive polymers (SRPs) that are sensitive to their environment or to externally applied impetus. This approach has the potential advantage of allowing simultaneous control of surface energy (e.g., through changes in hydrogen bonding) and topography (e.g., through local changes in polymer swelling).[1] Dynamic control of surface energy is of interest in control of wettability,[2] molecular adsorption,[3] adhesion,[4] and biocompatibility.[5] Control of nanotopography is also important in these areas, because of its capacity for synergistic amplification of surface phenomena and because of its ability to influence steric interactions in molecular transport and surface reactivity. We report a convenient experimental system wherein a versatile nanostructured surface based on nanoporous aluminum oxide formed via anodization is modified by a brush of poly(*N*-isopropyl acrylamide) (PNIPAAm), a well-studied SRP, with thickness comparable to the surface corrugation. This experimental system is demonstrated to allow direct correlation of changes in surface energy and nanotopography on macroscopic surface phenomena such as wettability. Much of the previous work on the use of SRPs to control interfacial properties has focused on the use of PNIPAAm because it is experimentally convenient: it exhibits a lower critical solubility temperature (LCST) in water at ~33 °C.[6] When PNIPAAm is displayed on a solid surface, this transition results in a change in the wettability of the surface above and below the LCST.

Beyond synthesis of dynamic nanostructured surfaces, the goals of this study are threefold. First, we demonstrate that polymer grafts prepared by surface-initiated atom transfer radical polymerization (ATRP) on nanotextured surfaces have a great influence on macroscopic wetting behavior. Recently, Sun et al. reported on the use of PNIPAAm grafted to textured surfaces formed by microlithography as a method for forming switchable superhydrophobic/superhydrophilic surfaces.[2] Our work here is different in that we show that such switching is achievable using nanotextured substrates in which changes in macroscopic wettability are likely due to not only change in hydrophobicity of the polymer as it passes through its transition temperature, but also because of changes in the nanoscopic topography of the surface associated with expansion and contraction of the grafted polymer layer. Second, we demonstrate direct visualization of changes in topography of nanostructured stimuli-responsive surfaces. Third, we develop a new method, based on principal components analysis, for quantitative correlation of changes in nanostructure, as visualized by atomic force microscopy (AFM), to changes in macroscopic water contact angles.

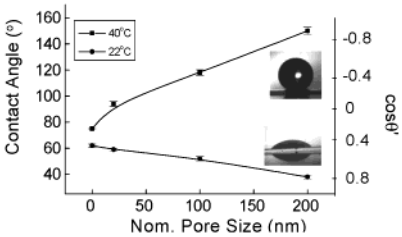

Figure 1. Water contact angle data (sessile drop) measured at 22 °C and 40 °C for PNIPAAm grafted to aluminum oxide surfaces with varying nominal pore size.

Commercial anodic aluminum oxide (AAO) membranes are good, inexpensive model systems by which to vary nanoscopic surface roughness. In this study, we used nonporous aluminum oxide and membranes with nominal pore sizes of 20, 100, and 200 nm (manuf. spec.) as model surfaces. We have previously published the synthetic method used to graft PNIPAAm to these surfaces via surface-initiated ATRP.[7] ATRP is an especially good method for surface modification because it is reproducible, does not lead to polymerization in the bulk solution (obviating the need for extensive extraction procedures to remove unattached polymer), and proceeds at relatively slow polymerization rates, leading to uniform coverage of textured surfaces and relatively low polydispersity. We have previously characterized the temperature-dependent wetting and swelling behavior of PNIPAAm brushes prepared by ATRP on flat surfaces via surface plasmon resonance and neutron reflectivity and have effectively modeled the temperature-induced transition using self-consistent field theory.[8] All polymer surfaces studied here were prepared under identical polymerization conditions, which yielded a brush of ~15 nm dry thickness (as measured by ellipsometry) on flat aluminum oxide.

Figure 1 presents wettability data for PNIPAAm grafted on the porous and nonporous surfaces at temperatures below and above the typical LCST observed for bulk solutions. In all cases change in temperature resulted in a change in water contact angle. Increasing the pore size of the substrate led to a gradual decrease in the contact angles measured at low temperature and a dramatic increase in contact angles measured at high temperature. Thus, the difference in contact angle measured at low and high temperature increased steadily, from ~13° to 112°.

We used AFM to examine the changes in the nanostructure of the PNIPAAm-modified AAO surfaces that result from variation in pore size and temperature. Figure 2 presents representative images for bare and PNIPAAm-modified AAO membranes at temperatures below and above the LCST. The images reflect changes in the nanostructure due to differences in template pore size, surface grafting of PNIPAAm, and change in temperature for the PNIPAAm-modified surfaces. Roughness factors (actual surface area/projected surface area) obtained from the images of the PNIPAAm surfaces

[†] Department of Chemical and Nuclear Engineering.
[‡] Department of Chemistry.

10.1021/ja047895q CCC: $27.50 © 2004 American Chemical Society

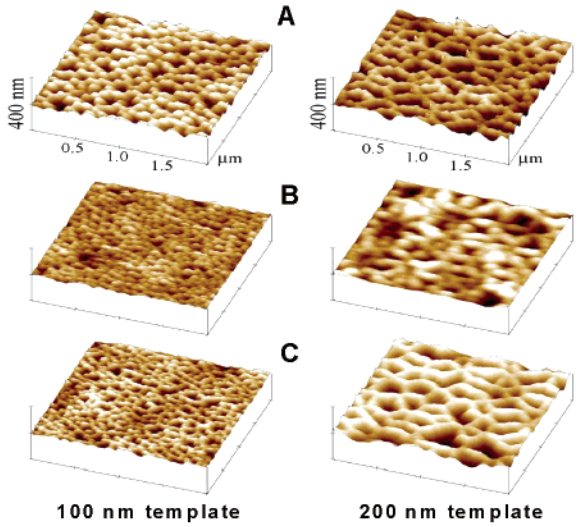

Figure 2. Representative topographical AFM images. (A) Bare AAO membranes (templates) in air. (B) PNIPAAm-grafted membranes in water at 25 °C. (C) PNIPAAm-grafted membranes in water at 40 °C.

increased steadily as the pore size increased and increased significantly upon increase in temperature for the 20 nm (1.15 at 25 °C to 1.24 at 40 °C) and 100 nm (1.23 to 1.33). The 200-nm samples did not show a dramatic difference in roughness factor at low and high temperatures, consistent with the expectation that changes in topography due to swelling and contraction of the thin polymer layer are less significant for larger pore sizes. Repeated imaging of samples at high and low temperature demonstrated reversible change in the nanostructure of the PNIPAAm-modified samples. No change in topography of dry samples was detected with temperature.

We attempted to correlate features in the nanostructure apparent in the AFM images with the measured macroscopic contact angles by implementing classic models of homogeneous and heterogeneous wetting of rough surfaces based on the Wenzel[9] and Cassie−Baxter[10] equations, respectively. Details of these equations and their use with AFM measured quantities are presented in the Supporting Information. In summary, direct use of roughness factors and solid−liquid interface area fractions (obtained by AFM) in the Wenzel equation allowed reasonable prediction of wetting at low temperature. In contrast, the Cassie−Baxter equations allowed only qualitative prediction of the contact angles measured at high temperature. This may be, in part, because the roughness factor obtained from AFM images may not be the true roughness of the surface and/or because the AFM images may not be sensitive to the solid−air interface in heterogeneous wetting.

We developed several multivariate statistical models based on principal components analysis (PCA) for correlating features in the AFM images with measured macroscopic contact angles. The best correlations were obtained using PCA of the histograms of AFM pixel intensities. Histograms contain important image statistics, such as mean, standard deviation, and skewness, which can be representative of surface morphology and, therefore, wettability. Another method that presented a meaningful relationship involved the use of PCA to correlate the Fourier transforms of the images. Figure 3A shows intensity histograms for representative images of the different types of PNIPAAm-modified porous AAO. PCA of these histograms reveals that 91% of their variation is described by the first principal component, which is centered around the mean gray level intensity (∼125) and 8% is described by the second principal component that has two peaks near the extremes of the gray level intensity values (∼50 and ∼165; see Supporting Information).

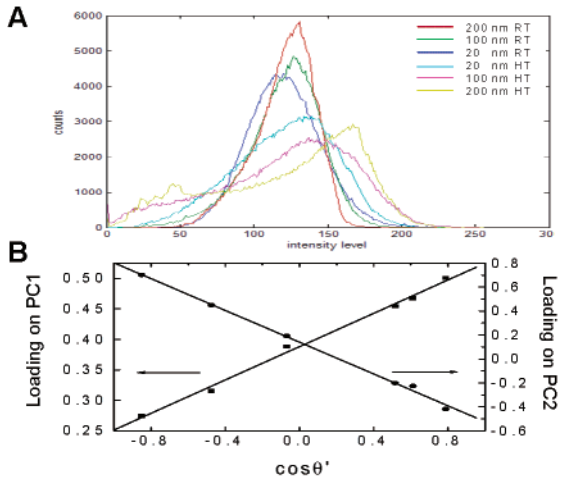

Figure 3. (A) Pixel intensity histograms for AFM images obtained for PNIPAAm-modified porous AAO surfaces at low and high temperature. (B) Correlation of the first and second principal components of the variation in the intensity histograms with macroscopic wettability.

Figure 3B demonstrates that these principal components are linearly correlated with the cosine of the contact angles, and thus AFM can be used in the quantitative prediction of a dynamic macroscopic property, e.g., the wettability.

The combined results show that it is possible to dynamically change crucial surface properties—the size of surface pores, the surface roughness, and the effective interfacial energy—on the nanometer scale using surface-grafted stimuli responsive polymers. The changes are controllable, reversible, and are reflected in large changes in contact angle and in easily visible changes in AFM images. Finally, the changes in macroscopic surface hydrophobicity can be quantitatively related to changes in surface nanostructure using principal component analysis.

Acknowledgment. This work was made possible through funding from the ARO, the NIH, the NSF, and the ONR.

Supporting Information Available: Contact angle measurements, correlation of data with wetting models, and principal components analysis of intensity histograms of AFM images. This material is available free of charge via the Internet at http://pubs.acs.org.

References

(1) Jones, D. M.; Smith, J. R.; Huck, W. T. S.; Alexander, C. *Adv. Mater.* **2002**, *14*, 1130−1134.

(2) Sun, T. L.; Wang, G. J.; Feng, L.; Liu, B. Q.; Ma, Y. M.; Jiang, L.; Zhu, D. B. *Angew. Chem., Int. Ed.* **2004**, *43*, 357−360.

(3) Huber, D. L.; Manginell, R. P.; Samara, M. A.; Kim, B. I.; Bunker, B. C. *Science* **2003**, *301*, 352−354.

(4) Tsuda, Y.; Kikuchi, A.; Yamato, M.; Sakurai, Y.; Umezu, M.; Okano, T. *J. Biomed. Mater. Res.* **2004**, *69A*, 70−78.

(5) Hoffman, A. S. *Adv. Drug Deliv. Rev.* **2002**, *54*, 3−12.

(6) Schild, H. G. *Prog. Polym. Sci.* **1992**, *17*, 163−249.

(7) Fu, Q.; Rao, G. V. R.; Ista, L. K.; Wu, Y.; Andrzejewski, B. P.; Sklar, L. A.; Ward, T. L.; Lopez, G. P. *Adv. Mater.* **2003**, *15*, 1262−1266.

(8) (a) Balamurugan, S.; Mendez, S.; Balamurugan, S. S.; O'Brien, M. J.; Lopez, G. P. *Langmuir* **2003**, *19*, 2545−2549. (b) Yim, H.; Kent, M. S.; Mendez, S.; Balamurugan, S. S.; Balamurugan, S.; Lopez, G. P.; Satija, S. *Macromolecules* **2004**, *37*, 1994−1997. (c) Mendez, S.; Balamurugan, S.; Balamurugan, S. S.; Lopez, G. P.; Yim, H.; Kent, M. S.; Curro, J. G.; McCoy, J. D. Proceedings of the American Institute of Chemical Engineers Annual Meeting; San Francisco, CA, Nov 16−21, 2003.

(9) Wenzel, R. N. *Ind. Eng. Chem.* **1936**, *28*, 988−994.

(10) Cassie, A. B. D.; Baxter, S. *Trans. Faraday Soc.* **1944**, *40*, 546−551.

JA047895Q